Thermo-mechanical behavior of the disc brake for varying the number of vanes

Nitin Kumar Aman [1], Sharifuddin Mondal[1]*

[1] Department of Mechanical Engineering, National Institute of Technology Patna, Bihar-800005, India

ARTICLE INFO	A B S T R A C T
	Brakes are a vital, prime, and accident preventive part of any motor vehicle. Brakes help in controlling the vehicle speed when needed by changing the kinetic energy and potential energy into thermal energy. In this work, we have found out temperature distribution, deformation distribution, equivalent stress distribution, and equivalent strain distribution by varying the number of vanes in a ventilated disc brake, considering the coupled thermal and structural field in transient conditions, and compared the results to find out the best possible design. We have considered the disc rotor's material as grey cast iron and the disc pad's material as carbon fiber reinforced carbon matrix. It has been found out that with an increase in the number of vanes, there is a reduction in the maximum deformation, maximum stress, and maximum strain and there is a slight increase in the maximum temperature during the whole simulation. A disc rotor with 18 vanes is found to be the best possible design among all 5 designs considered in this paper.

*Corresponding Author:
Email Address: sharifuddin@nitp.ac.in
https://doi.org/10.22068/ase.2021.592

1. Introduction

Brakes are very important parts of any motor vehicle. Some roads are uneven, some are slippery, wet or dry, some have stiff curves, some are inclined and many more but brakes have to work in all this circumstances. Brakes help in decelerating the vehicle speed on a level road, controlling the vehicle speed during downhill and stopping the vehicle when needed by changing the kinetic energy and potential energy (during downhill) into thermal energy via the friction generated between the brake disc and brake pad in case of disc brake and also in holding the vehicle in stagnant position [1].Major reason for considering the disc brake is due to its ability to withstand high temperature rise up to 1072 K to 1172 K with modest fade.Structural as well as thermal analysis of disc brake is represented extensively and separately but very few studies are conducted on the thermo-structural coupled analysis and no study was found on the coupled field transient analysis. Belhocine and Abdulla [2] presented a comparative analysis of the two different design and three different materials of the disc rotor. Pevec et. al.[3] performed computational fluid dynamics (CFD) stimulation of disc rotor to calculate the heat transfer coefficient on the wall of the rotor and estimate the temperature distribution in the rotor.Jian and Yan [4] investigated transient temperature distribution of the disc brake under hard braking condition by developing a thermo-structural coupled model. Guo et. al.[5] built a representative volume element (RVE) model to examine the coefficients of thermal expansion and conductivity of carbon/carbon composites. Yan et. al. [6] reported the effects of vane outlet angle on curved vane disc brake and found that the increasing the vane angle from 45˚ to 130˚ improves the cooling up to 16 %. Yan et. al. [7] found out that cross-drilled brake disc have 22-27% higher overall Nusselt number in the speed range of 200-1000 RPM. Yevtushenko et. al. [8] proposed a mathematical model of the disc brake

to evaluate the temperature field distribution by considering the thermal barrier cooling (TBC). Study by Belhocine and Bouchetara [9] suggested that the Von-mises stress and total deformation increase in a significant manner when both structural and thermal aspects are considered together. Chen and Kienhofer [10] conducted experimental study and found out that the compressive stresses are centralized around the disc/pad contact interface and are insignificant elsewhere during the clamp load test and for the applied torque load test, the shear stresses are scattered throughout the circumference in the disc but maximum occurred at the disc/pad interface. Kishore and Vineesh [11] found that the maximum temperature rise of 215˚C in disc of diameter 290 mm in the radial direction while applying brakes at 160kmph to stop the vehicle at 60 % of braking time. Jian et. al. [12] investigated thermal behavior of ventilated brake disc (VBD) by embedding heat pipes and found out 36.67% and 21.43% improvement in thermal uniformity and 12.62% and 18.90% increase in heat dissipation during experiment and under stimulation, an increase of 10.77% and 13.66% in temperature uniformity and an increase of 12.87% and 3.41% in heat dissipation during single cycle brakes and continuous downhill braking. Yevtushenko et. al. [20] experimentally studied three types of brake pads namely metallic fibers,steel and copper. Dynamometer test was performed to determine the frictional features of the materials and to examine the effect of metal fibers on the temperature evolution. It has been found that despite high thermal conductivity, metal fibers did not lower temperature of the disc brake. Chen et. al. [21] conducted the field test measurement and a finite element analysis of disc brake squeal and found that the occurrence propensity of the brake squeal related to the variation of braking air pressure against time.The objective of this work is to find out effect on the temperature distribution, deformation distribution, equivalent stress distribution and

equivalent strain distribution on varying the number of vanes in ventilated disc brake by considering the coupled thermal and structural field in transient conditions.

Rest of the paper is organized as follows. In section 2, methodology of analysis is presented. Results and discussion are made in section 3. Finally concluding remarks are listed in section 4.

2. Methodology

2.1. Geometry

Standard disc rotor dimensions have been taken for this paper as shown in Table 1.

2.2. Materials

Material selected for disc rotor is grey cast iron due to its metallurgical stability behavior, thermal transportable properties, lower cost and easy manufacturability [13-16] and for disc pad is carbon fiber reinforced carbon matrix because of its long service life and smooth braking [17-18]. The properties of gray cast iron are shown in Table 2 while the properties of carbon-carbon composite are tabulated in Table 3.

2.3. Mesh

During meshing, tetrahedral is selected as element type as it is the best suitable element type for a complex geometry. No significant variation in results is seen by further reducing the mesh size, so it is taken as 0.5 mm for all the parts of the models.

Table. 1. Design Parameters of disc brake

Design Parameters of disc brake	
Outer diameter of disc rotor	420 mm
Inner diameter of disc rotor	125 mm
Disc thickness	15 mm both sides,15 mm vented
Weight of cars (with passengers)	2215 kg

Table. 2. Properties of grey cast iron

Properties of grey cast iron	
Density	7200 kg/m^3
Young Modulus	1.1e+ 11 Pa
Poisson's Ratio	0.28
Thermal Conductivity	52 W/m.°C
Specific Heat Constant Pressure	447 J/kg.°C

Table. 3. Properties of Carbon matrix, carbon fiber reinforced (Vf:50%), composite

Properties of Carbon matrix, carbon fiber reinforced (Vf:50%), composite	
Density	1700 kg/m^3
Young Modulus	9.487e+ 10 Pa
Poisson's Ratio	0.3198
Thermal Conductivity	26.27 W/m.°C
Specific Heat Constant Pressure	756J/kg.°C

Table. 4. Braking distance and deceleration data

Braking Distance and Deceleration		
Speed	**Braking Distance(m)**	**Time to stop(sec)**
100 km/hr. – 0 km/hr.	31.4	2.4
200 km/hr. – 0 km/hr.	114	6.1
300 km/hr. – 0 km/hr.	247	13.1
400 km/hr. – 0 km/hr.	491	32.6
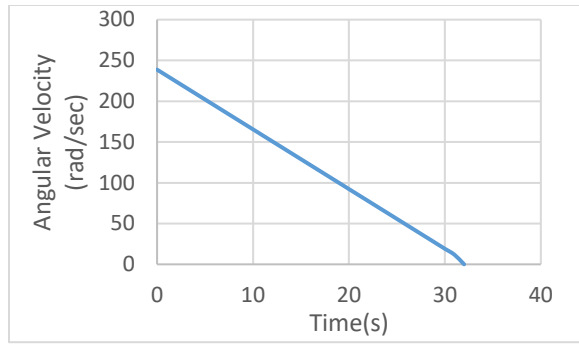
Fig. 1. Plot between angular velocity versus time

Fig. 2. The front wheel rotor system

2.4.Boundary Conditions

Both initial and. ambient temperatures are taken as 22°C. Analysis is done in 150 steps and in each steps a minimum of 10 and maximum of 100 sub-steps is taken. The braking distance and deceleration data is shown in Table 4.

2.4.1. Angular Velocity

Angular velocity is assumed to vary linearly with respect to time. Below graph (Figure 1) shows the variation of angular variation with respect to time. Data has been tabulated and inserted as boundary condition in ANSYS.

2.4.2. Pressure

Pressure applied by disc pad on disc rotor is 1 MPa. A schematic diagram of the front wheel rotor system is shown in Figure 2 where ɱ is the mass of the vehicle with passengers,g is the acceleration due to gravity (9.81m/s2), µroad is the coefficient of friction between type and road, Rtyre is the radius of tyre, Rrotor is the radius of disc rotor, TTire is the frictional force between the road and tire and W is the normal force due to weight of vehicle.
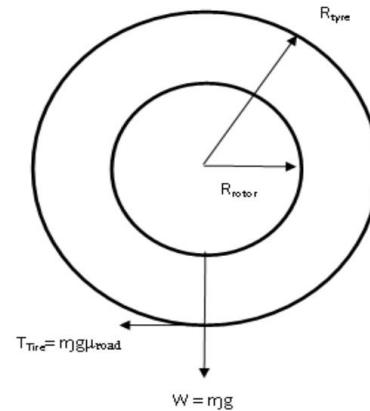
Front brake is considered here for calculation as it bears the maximum load during braking. Kinetic Energy and Potential Energy is given by below equation in a single disc where E_(n Dissipated) represents the total energy required to stop the vehicle from a particular speed to zero, ʋ _0 represents the velocity of the vehicle before applying brake, k is the ratio of kinetic energy absorbed by one of the front wheel,δ is the angle of inclination of road and d_s is the stopping distance of the vehicle.

$$E_{n\ Dissipated} = \frac{1}{2}k\textrm{ɱ}\upsilon_0^2 + d_s\textrm{ɱ}g\sin\delta \qquad (1)$$

$$d_s = \frac{v_0^2}{2a} \qquad (2)$$

Combining Equation (1) and (2), we get,

$$E_{n\ Dissipated} = \frac{1}{2}k\textrm{ɱ}\upsilon_0^2 + \frac{v_0^2}{2a}\textrm{ɱ}g\ sin\delta \qquad (3)$$

The power throw away from each rotor face is equivalent to the heat flux into the rotor face. In equation (4), (5) and (6) ,P_(w Dissipated)represents total power required to stop the vehicle from a particular speed to zero,ƭ represents time taken to stop the vehicle,F_(r rotor)is the force on the rotor,V_rotoris the velocity of the rotor and a

is the acceleration of the vehicle before applying brake.

$$E_{n\,Dissipated} = \int P_{w\,Dissipated}\, \mathfrak{t}\, d\mathfrak{t} = \int 2F_{r\,rotor}V_{rotor}\mathfrak{t}\, d\mathfrak{t} \quad (4)$$

$$\frac{1}{2}km\upsilon_o^2 + \frac{\upsilon_o^2}{2a}mgsin\delta = KE_{n\,Dissipated} = \int P_{w\,Dissipated}\, \mathfrak{t}\, d\mathfrak{t} = \int 2F_{r\,rotor}V_{rotor}\mathfrak{t}\, d\mathfrak{t} \quad (5)$$

However, from kinematics, we have

$$V_{Vehicle} = \upsilon_o - a\mathfrak{t} \quad (6)$$

$$a = \frac{\upsilon_o}{\mathfrak{t}_{stop}}$$

$$\frac{V_{Vehicle}}{R_{Tyre}} = \frac{V_{rotor}}{R_{rotor}}$$

$$\frac{1}{2}km\upsilon_o^2 + \frac{\upsilon_o^2}{2a}mgsin\delta = \int 2F_{rotor}V_{rotor}\mathfrak{t}\, d\mathfrak{t} \quad (7)$$

$$= 2F_{rotor}\frac{R_{rotor}}{R_{tyre}}\left(\upsilon_0\mathfrak{t}_{stop} - \frac{1}{2}\left\{\frac{\upsilon_o}{\mathfrak{t}_{stop}}\right\}\mathfrak{t}_{stop}^2\right)$$

$$F_{r\,rotor} = \frac{\frac{1}{2}km\upsilon_o^2 + \frac{\upsilon_o^2}{2a}mgsin\delta}{2F_{rotor}\frac{R_{rotor}}{R_{tyre}}\left(\upsilon_0\mathfrak{t}_{stop} - \frac{1}{2}\left(\frac{\upsilon_o}{\mathfrak{t}_{stop}}\right)\mathfrak{t}_{stop}^2\right)} \quad (8)$$

When braking on straight path with no inclination, δ=0, k is calculated as approximately 0.30.

$$F_{d\,Disc} = \frac{(30\,\%)\frac{1}{2}m\upsilon_o^2}{2F_{r\,rotor}\frac{R_{rotor}}{R_{tyre}}\left(\upsilon_0\mathfrak{t}_{stop} - \frac{1}{2}\left(\frac{\upsilon_o}{\mathfrak{t}_{stop}}\right)\mathfrak{t}_{stop}^2\right)} \quad (9)$$

$$F_{d\,disc} = 1934.4068\,N$$

$$\omega = \frac{\upsilon_o}{R_{tyre}} = 238.68\,rad/sec \quad (10)$$

$$P_r = \frac{F_{disc}}{A_c * \mu} = 1\,MPa \quad (11)$$

In above equations, ω is the angular velocity of the vehicle before applying brake, P_r is the pressure applied on the brake rotor by the brake pad,F_disc is the force applied on the brake disc and A_c is the area swept by the brake pad on the brake disc.

2.4.3. Heat Flux

Heat is generated by friction between the brake rotor and brake pads. This heat enters into the disc rotor. As per the formula derived, it depends upon the velocity. Therefore, a change in velocity means a change into value of heat flux. Heat flux is calculated by formula derived [2], where q_o represents heat flux generated due to friction between brake disc and brake pad and Ø is the ratio of load on the particular wheel to total load of all wheels. Other symbols have the same meaning as above described.

Heat flux vs time is plotted in Figure 3.

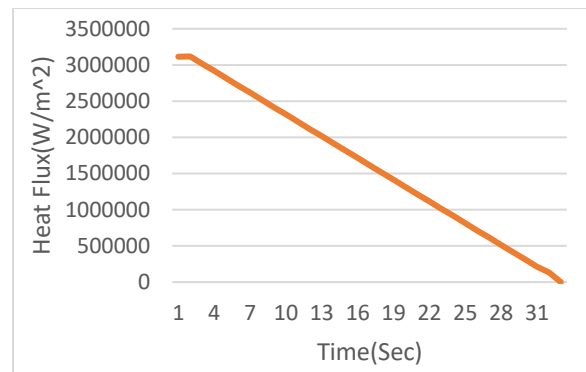$$P_r = \frac{F_{disc}}{A_c * \mu} = 1\,MPa \quad (12)$$

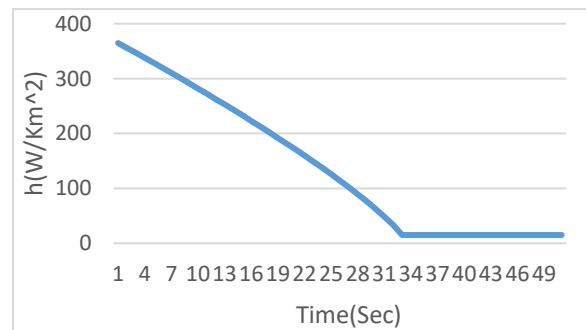Fig. 3. Plot between heat flux versus time.

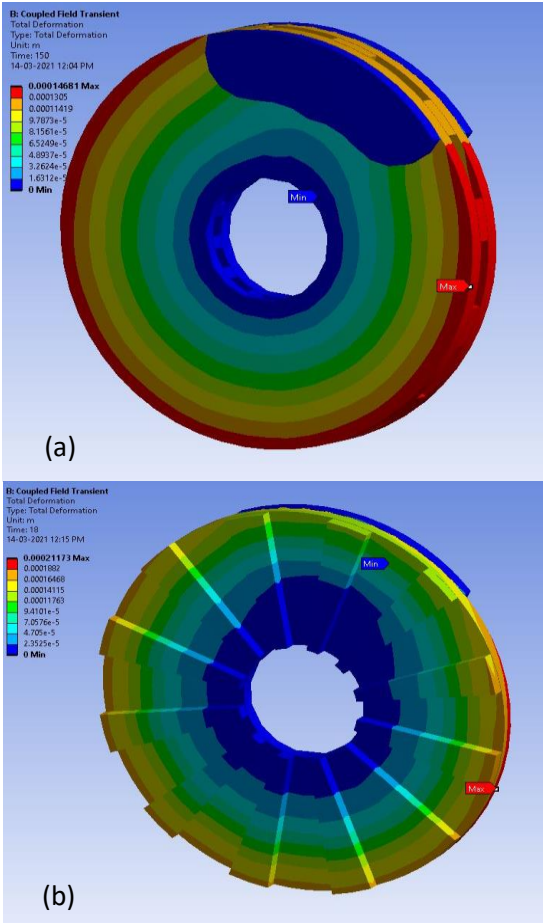Fig. 4. Plot between h (convective heat transfer coefficient) versus time.

3705

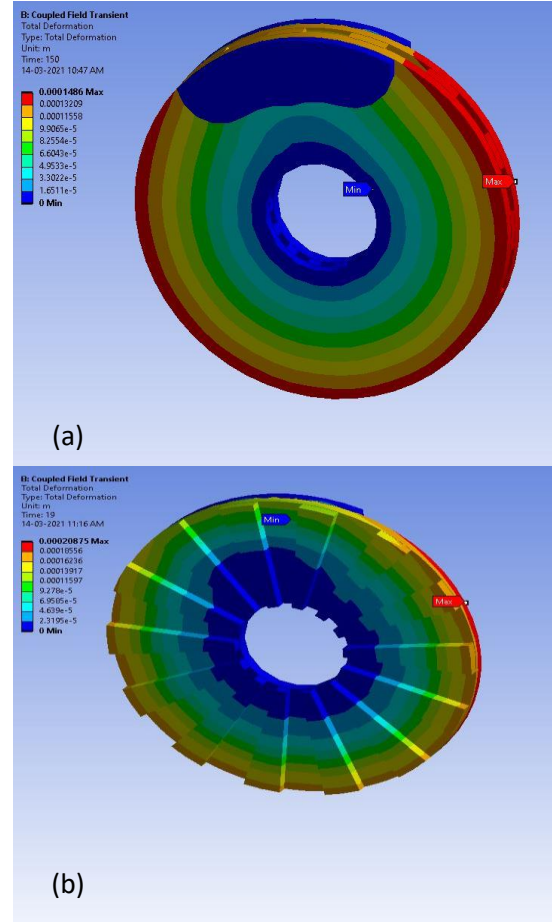Fig. 5. Deformation distribution in disc brake with 12 vanes (a)150th Sec(b) 18th Sec.

Fig. 6. Deformation distribution in disc brake with 14 vanes (a)150th Sec (b) 19th Sec

2.4.4. Convection

The effect of radiation is neglected in this analysis, as there is negligible effect on the heat dissipation from the disc rotor.

Coefficient of heat transferfor the vented disc brakecalculated by the formula derived [19] where h_Ris the coefficient of heat transfer for the vented disc brake,d_h is the hydraulic diameter of the fluid flow,l is the length of the disc rotor assuming flat plate condition,Re represents reynolds number, Pr represents prandtl number and K_a is the diameter of the rotor. Convective heat transfer coefficient (h_R) vs time is shown in Figure 4.

$$h_R = 0.023\left[\left(1+\left(\frac{d_h}{l}\right)\right)^{0.67}\right]Re^{0.8}Pr^{0.33}*\left(\frac{K_a}{d_h}\right) W/Km^2$$
(13)

3. Results & Discussion

Vented disc rotor with different numbers of vanes has been stimulated with the above boundary conditions. In this thesis, 12, 14, 16 and 18 vanes of same size are selected for the analysis based. Selection of number of vanes is based on the actual numbers of vanes used in disc brake. Transient Coupled field analysis is performed in the Ansys for 150 Sec.

3.1.Deformation Distribution

3.1.1. 12 Vanes

After a stimulation of 150 seconds in the disc with 12 vanes, it is seen in Figure 5 (a) that a maximum of 0.1468 mm deformation occurs at the edge of the disc and

3706   Automotive Science and Engineering

negligible deformation occurs at the inner edge. During the stimulation, it is seen in Figure 5 (b) that a maximum deformation of 0.2117 mm occurs at 18th second.
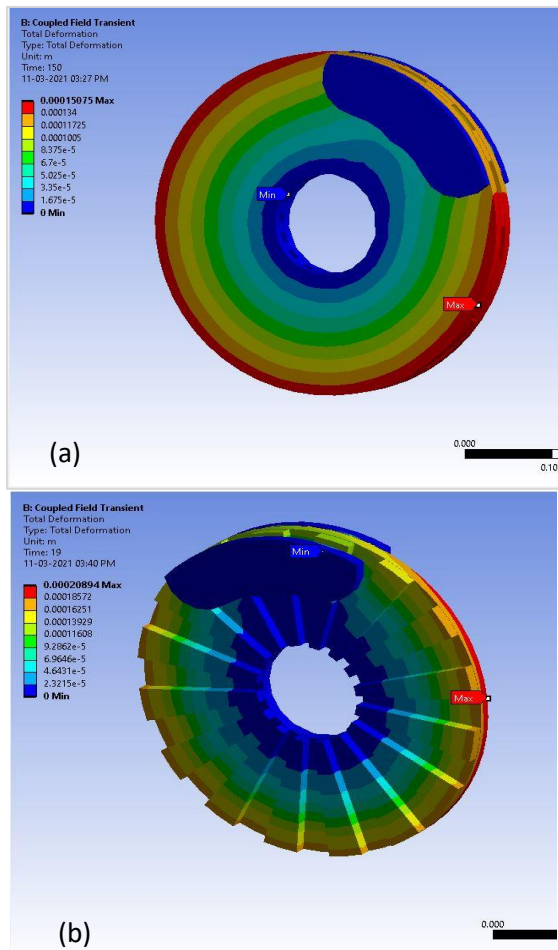
After a stimulation of 150 seconds in the disc with 12 vanes, it is seen in Figure 5 (a) that a maximum of 0.1468 mm deformation occurs at the edge of the disc and negligible deformation occurs at the inner edge. During the stimulation, it is seen in Figure 5 (b) that a maximum deformation of 0.2117 mm occurs at 18th second.


(a)

(b)

Fig. 7. Deformation distribution in disc brake with 16 vanes (a)150th Sec (b) 19thSec

3.1.2. 14 Vanes

After a stimulation of 150 seconds in the disc with 14 vanes, it is seen in Figure 6 (a) that a maximum of 0.1486 mm deformation occurs at the edge of the disc and negligible deformation occurs at the inner edge. During the stimulation, it is seen in Figure 6 (b) that a maximum deformation of 0.2087 mm occurs at 19th second.

3.1.3. 16 Vanes

After a stimulation of 150 seconds in the disc with 16 vanes, it is seen in Figure 7 (a) that a maximum of 0.1507 mm deformation occurs at the edge of the disc and negligible deformation occurs at the inner edge. During the stimulation, it is seen in Figure 7 (b) that a maximum deformation of 0.2089 mm occurs at 19th second.

(a)

(b)
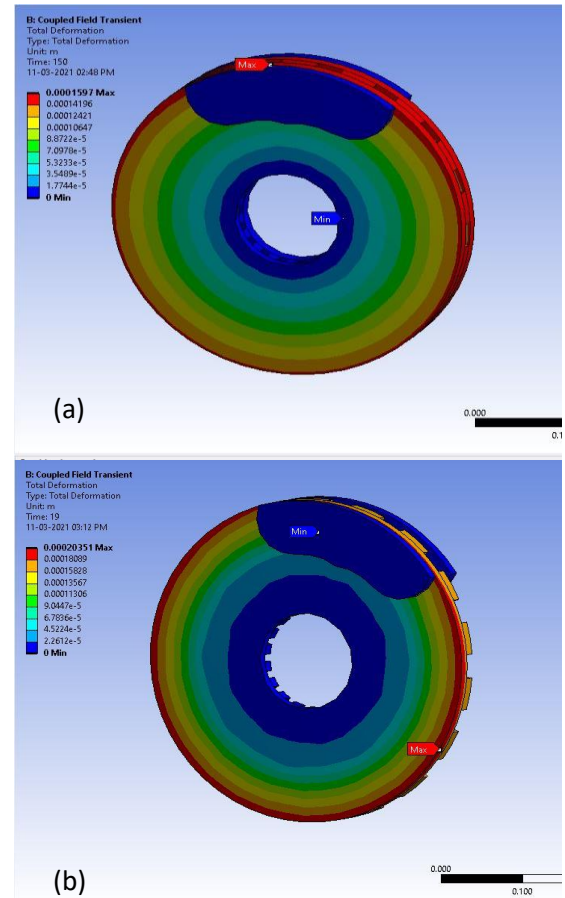
Fig. 8 Deformation distribution in disc brake with 18 vanes (a)150th Sec (b) 19th Sec
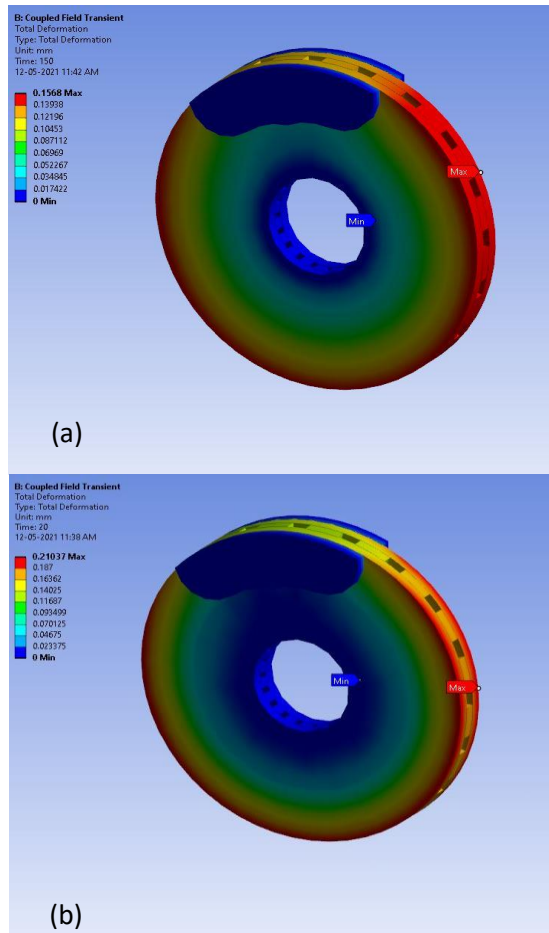
(a)

(b)

Fig. 9 Deformation distribution in disc brake with 20 vanes (a)150th Sec (b) 20th Sec.

Table. 5. Comparison of deformations of different vanes

No of Vanes	Deformation at 150 sec (mm)	Maximum Deformation (mm)	Minimum Deformation (mm)	% Change in Max. Deformation
12	0.1468	0.2117	0	0
14	0.1468	0.2087	0	-1.41709967
16	0.1507	0.2089	0	-1.32262636
18	0.1579	0.2035	0	-3.87340576
20	0.1568	0.21037	0	-0.62824752

3.1.4. 18 Vanes

After a stimulation of 150 seconds in the disc with 18 vanes, it is seen in Figure 8 (a) that a maximum of 0.1579 mm deformation occurs at the edge of the disc and negligible deformation occurs at the inner

edge. During the stimulation, it is seen in Figure 8 (b) that a maximum deformation of 0.2035 mm occurs at 19th second.

3.1.5. 20 Vanes

After a stimulation of 150 seconds in the disc with 20 vanes, it is seen in Figure 9 (a) that a maximum of 0.1568 mm deformation occurs at the edge of the disc and negligible deformation occurs at the inner edge. During the stimulation, it is seen in Figure 9 (b) that a maximum deformation of 0.21037 mm occurs at 20th second.

3.1.6. Comparisons

From the below graph (Figure 10), it can be seen that as the number of vanes increases from 12 vanes to 18 vanes, maximum deformation decreases but after that it starts increasing. It is found that maximum deformation occurs in disc with 12 vanes. As the number of vanes increases from 12 to 18, there is minor reduction in the maximum deformation but, from 18 to 20, slight increase in maximum deformation is observed during the whole stimulation. From Table 5, it is clear that disc rotor with 18 vanes has lowest maximum deformation among all 5 designs and has 3.87% less maximum deformation than disc rotor with 12 vanes.

3.2.Stress Distribution

3.2.1. 12 Vanes

After a stimulation of 150 seconds in the disc with 12 vanes, it is seen in Figure 11 (a) that a maximum of 148.3 MPa von-mises stress occurs at the inner edge of the disc and a minimum of 11.35 MPa occurs at the point indicated in below image.
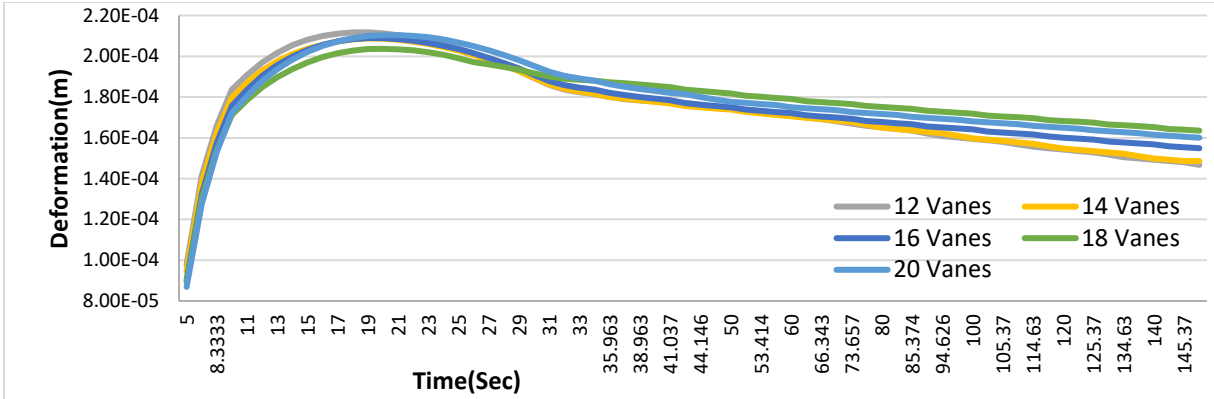
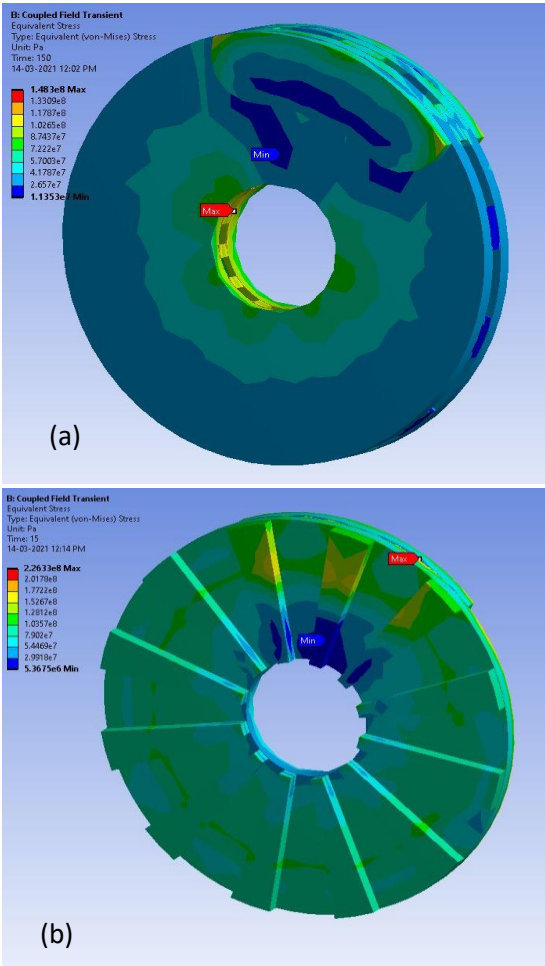Fig. 10 Plot between deformations versus time in different vane

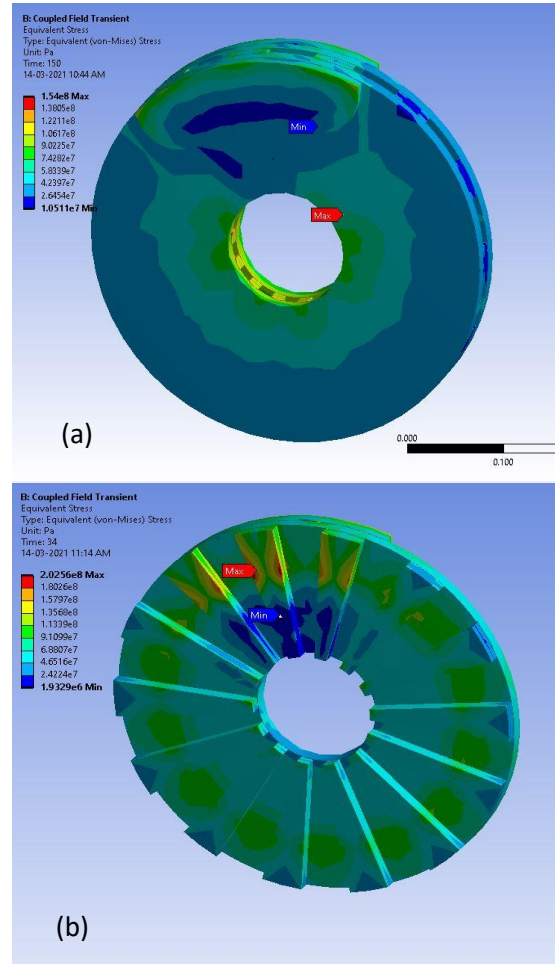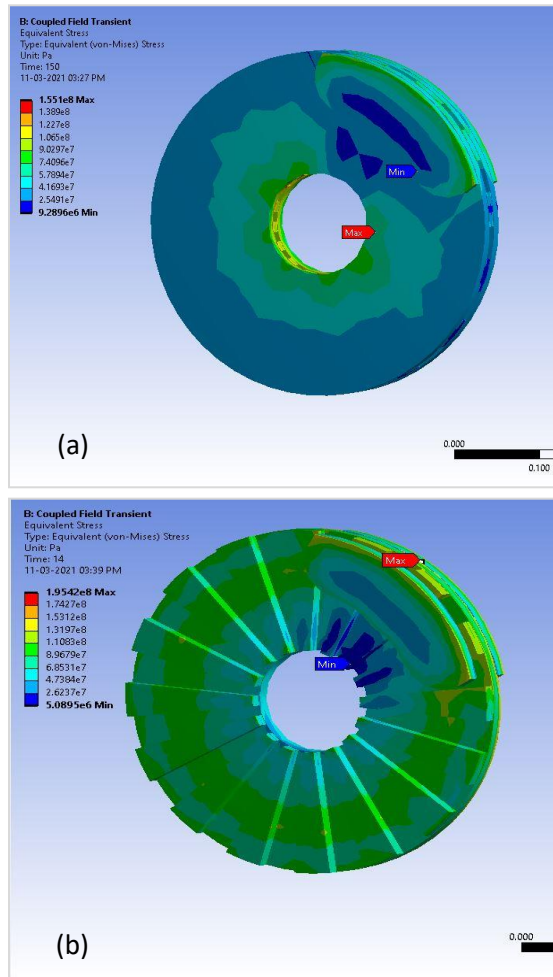Fig. 11. Stress distribution in disc brake with 12 vanes (a)150th Sec (b)15thSec
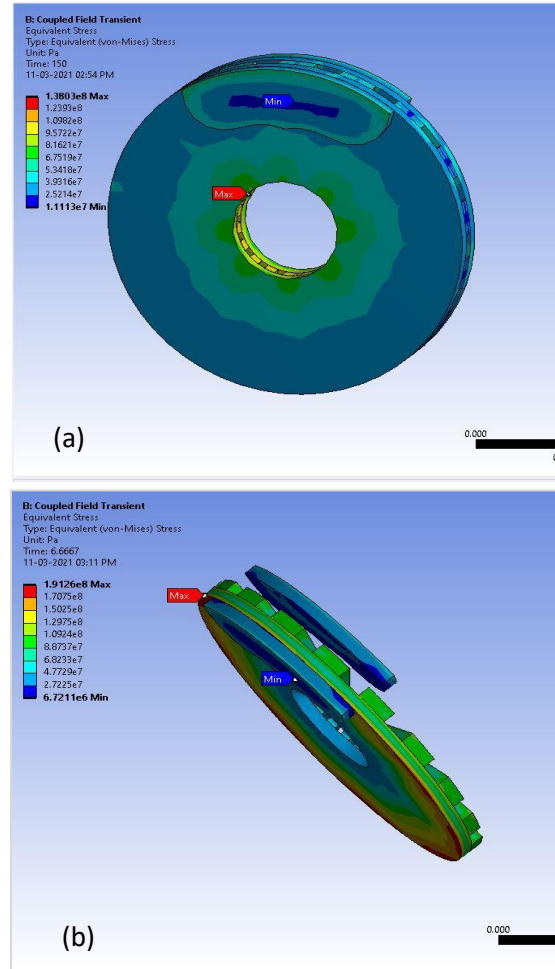

Fig. 12. Stress distribution in disc brake with 14 vanes (a)150th Sec (b) 34th Sec

3.2.2. 14 Vanes

After a stimulation of 150 seconds in the disc with 14 vanes, it is seen in Figure 12(a) that a maximum of 154 MPa von-mises

stress and a minimum of 10.51 MPa occur at the point indicated in below image. During the stimulation, it is seen in Figure 12(b) that a maximum von-mises stress of 202.56 MPa

and a minimum of 1.93 MPa occur at 34th second.

(a)

(b)

Fig. 13. Stress distribution in disc brake with 16 vanes (a) 150th Sec (b) 14th Sec

3.2.3. 16 Vanes

After a stimulation of 150 seconds in the disc with 16 vanes, it is seen in Figure 13 (a) that a maximum of 155.51 MPa von-mises stress and a minimum of 9.26 MPa occur at the point indicated in below image. During the stimulation, it is seenin Figure 13 (b) that a maximum von-mises stress of 195.42 MPa and a minimum of 5.089 MPa occur at 14th second.

(a)

(b)

Fig. 14. Stress distribution in disc brake with 18 vanes (a)150th Sec (b) 6.66th Sec

3.2.4. 18 Vanes

After a stimulation of 150 seconds in the disc with 18 vanes, it is seen in Figure 14 (a) that a maximum of 138.03 MPa von-mises stress and a minimum of 11.11MPa occur at the point indicated in below image. During the stimulation, it is seen in Figure 14 (b) that a maximum von-mises stress of 191.26 MPa and a minimum of 6.72 MPa occur at 6.66th second.

3.2.5. 20 Vanes

After a stimulation of 150 seconds in the disc with 20 vanes, it is seen in Figure 15

(a) that a maximum of 164.63 MPa von-mises stress and a minimum of 5.26 MPa occur at the point indicated in below image. During the stimulation, it is seen in Figure 15 (b) that a maximum von-mises stress of 193.41 MPa and a minimum of 3.015 MPa occur at 6.66th second.

Table. 6. Comparison of stresses of different vanes

No of Vanes	Stress at 150 sec (MPa)		Maximum Stress (MPa)	Minimum Stress (MPa)	% Change in Maximum Stress
	Max	Min			
12	148.3	11.35	226.33	5.36	0
14	154	10.51	202.56	1.93	-10.5023638
16	155.51	9.26	195.42	5.089	-13.6570494
18	138.03	11.11	191.26	6.72	-15.4950736
20	164.63	5.261	193.41	3.015	-14.54513321

(a)

(b)
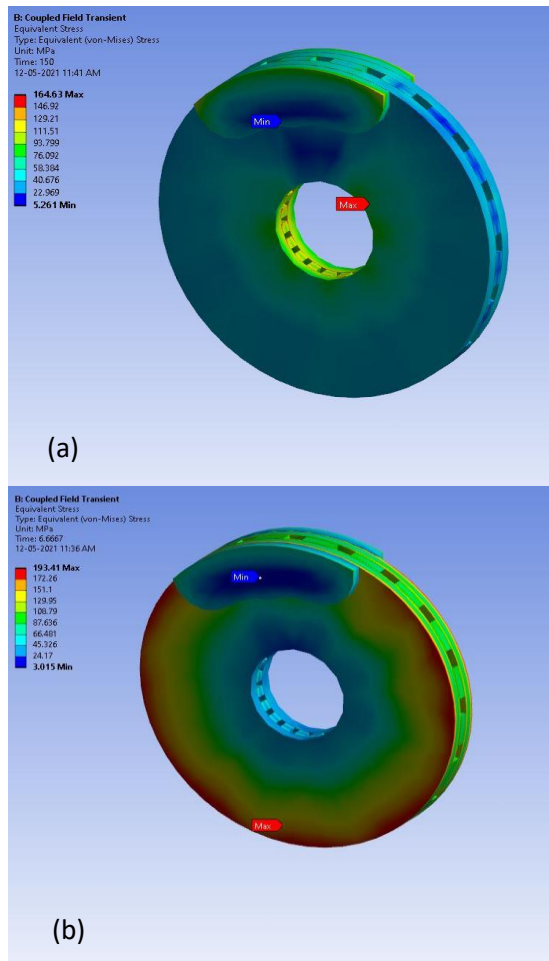
Fig. 15. Stress distribution in disc brake with 20 vanes (a) 150th Sec (b) 6.66[th] Sec

3.2.6. Comparisons

From the below graph (Figure 16), it can be seen that as the number of vanes increases from 12 to 18, maximum equivalent stress decreases, but after that it starts increasing. It is found that maximum stress occurs in disc with 12 vanes. As the number of vanes increases from 12 to 18, there is reduction in the maximum stress but, from 18 to 20, an increase in maximum stress is observed during the whole stimulation. From Table 6, it is clear that disc rotor with 18 vanes has lowest maximum stress among all 5 designs and has 15.49% less maximum stress than disc rotor with 12 vanes.

3.3. Strain Distribution

3.3.1. 12 Vanes

After a stimulation of 150 seconds in the disc with 12 vanes, it is seen in Figure 17 (a) that a maximum of 0.001348 von-mises strain and a minimum of 0.00017883 occur at the point indicated in below image. During the stimulation, it is seen in Figure 17 (b) that a maximum von-mises strain of 0.002125 and a minimum of 0.0001064 occur at 15th second.

3.3.2. 14 Vanes

After a stimulation of 150 seconds in the disc with 14 vanes, it is seen in Figure 18 (a) that a maximum of 0.0014 von-mises strain and a minimum of 0.0002182 occur at the point indicated in below image. During the stimulation, it is seen in Figure 18 (b) that a maximum von-mises strain of 0.018938 and a minimum of 8.28e-5 occur at 14th second.

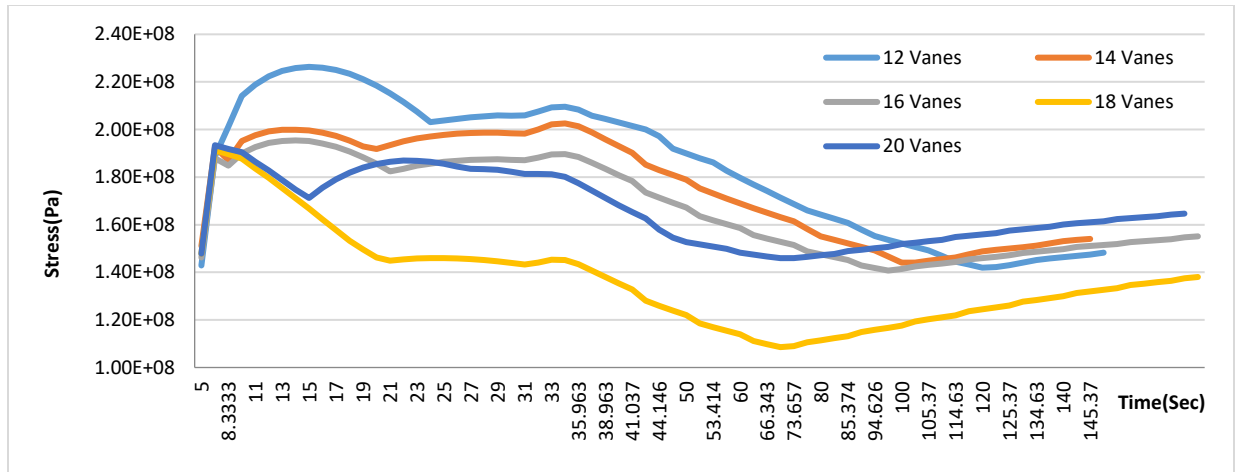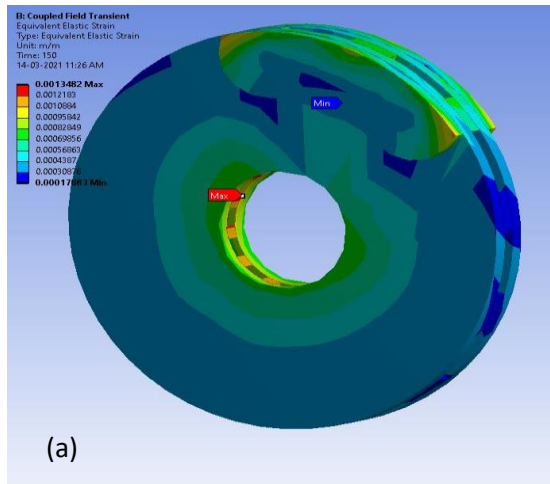**Thermo-mechanical behavior of the disc brake for varying the number of vanes**
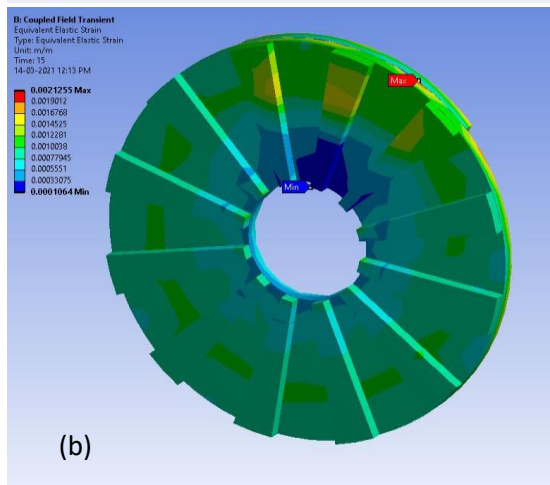

Fig. 16. Plot between stresses versus time in different vanes
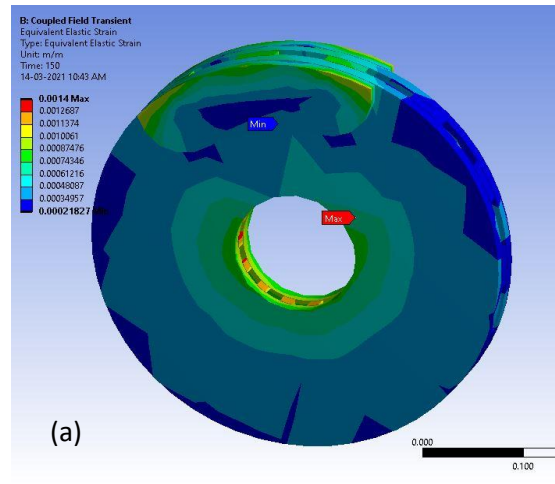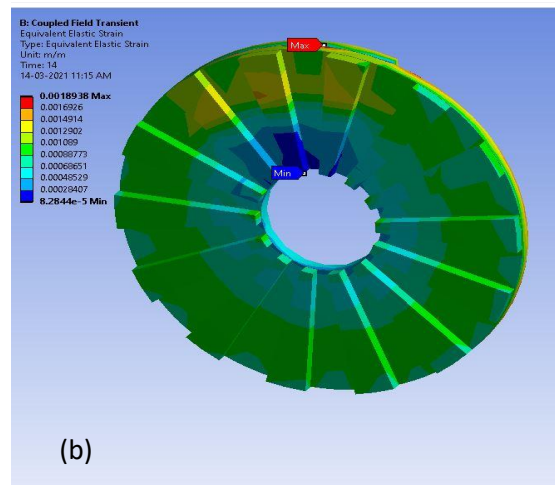

(a)

(b)

Fig. 17. Strain distribution in disc brake with 12 vanes (a)150th Sec (b)15th Sec

(a)

(b)

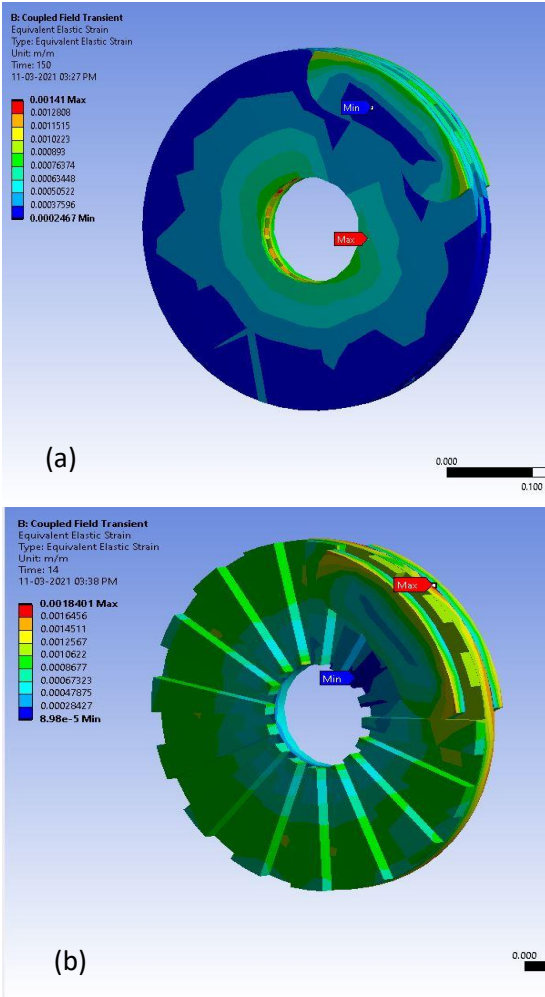Fig. 18. Strain distribution in disc brake with 14 vanes (a)150th Sec (b)14th Sec

(a)

(b)

Fig. 19. Strain distribution in disc brake with 16 vanes (a)150ᵗʰ Sec (b)14ᵗʰ Sec

3.3.3. 16 Vanes

After a stimulation of 150 seconds in the disc with 16 vanes, it is seen in Fig. 19(a) that a maximum of 0.00141 von-mises strain and a minimum of 0.0002467 occur at the point indicated in below image. During the stimulation, it is seen in Fig. 19(b) that a maximum von-mises strain of 0.0184 and a minimum of 8.98e-5 occur at 14ᵗʰ second.

3.3.4. 18 Vanes

After a stimulation of 150 seconds in the disc with 18 vanes, it is seen in Fig. 20(a) that a maximum of 0.0012548 von-mises
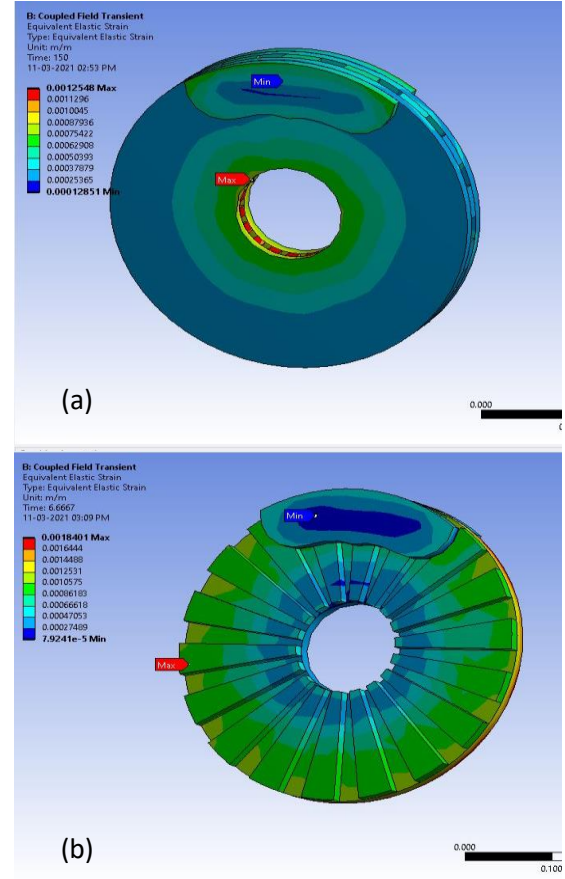

(a)

(b)

Fig. 20. Strain distribution in disc brake with 18 vanes (a)150ᵗʰ Sec (b) 6.66ᵗʰ Sec

strain and a minimum of 0.0001285 occur at the point indicated in below image. During the stimulation, it is seen in Fig. 20(b) that a maximum von-mises strain of 0.0184 and a minimum of 7.92e-5 occur at 6.6ᵗʰ second.

3.3.5. 20 Vanes

After a stimulation of 150 seconds in the disc with 20 vanes, it is seen in Fig. 21(a) that a maximum of 0.0014966 von-mises strain and a minimum of 0.00021175 occur at the point indicated in below image. During the stimulation, it is seen in Fig. 21(b) that a maximum von-mises strain of 0.0197 and a minimum of 9.617e-5 occur at 22th second.
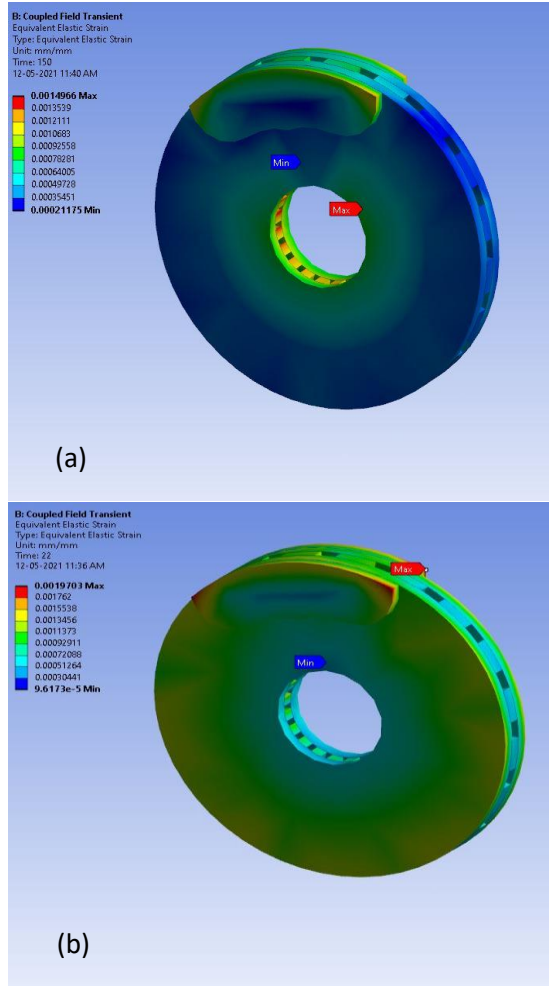
3713

(a)

(b)

Fig. 21. Strain distribution in disc brake with 18 vanes (a)150th Sec (b) 22th Sec

3.3.6. Comparisons

From the below graphs (Figure 22), it can be seen that as the number of vanes increases from 12 to 18, maximum equivalent strain decreases, but after that it starts increasing. It is found that maximum strain occurs in disc with 12 vanes. As the number of vanes increases from 12 to 18, there is reduction in the maximum strain but, from 18 to 20, an increase in maximum strain is observed during the whole stimulation. From Table 7, it is clear that disc rotor with 18 vanes has lowest maximum strain among all 5 designs

and has 13.61% less maximum strain than disc rotor with 12 vanes.

3.4.Temperature Distribution

3.4.1. 12 Vanes

After a stimulation of 150 seconds in the disc with 12 vanes, it is seen in Figure 23 (a) that a maximum of 121.37 °C and a minimum 59.71 °C occur at the point indicated in below image. During the whole stimulation, it is seen in Figure 23 (b) that a maximum 268.01 °C and a minimum of 25°C occur at 12th second.

3.4.2. 14 Vanes

After a stimulation of 150 seconds in the disc with 14 vanes, it is seen in Figure 24 (a) that a maximum of 121.75 °C and a minimum 60.217 °C occur at the point indicated in below image. During the whole stimulation, it is seen in Figure 24 (b) that a maximum 268.50 °C and a minimum of 25°C occur at 12th second.

Table. 7. Comparison of strains of different vanes

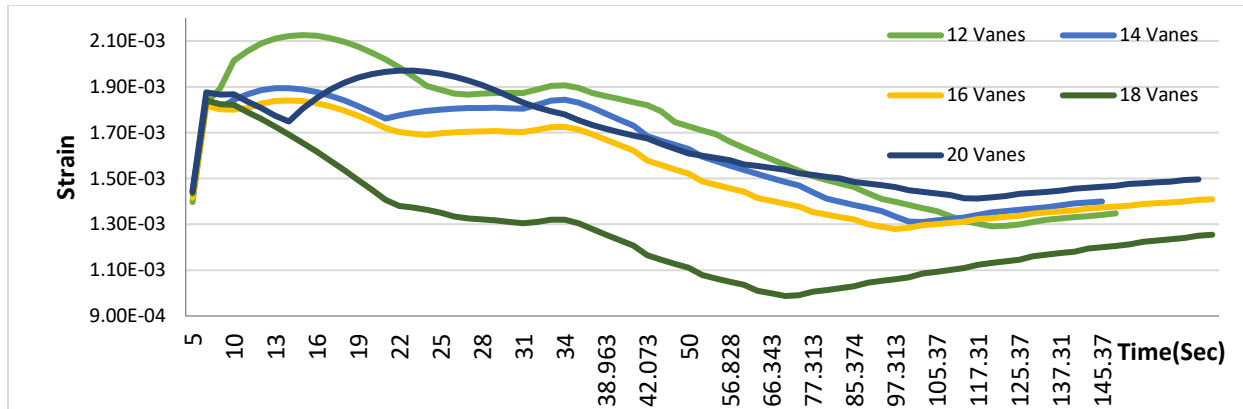| No of Vanes	Strain at 150 sec		Maximum Strain	Minimum Strain	% Change in Maximum Strain
	Max	Min			
12	0.001348	0.0001788	0.002125	10.64e-5	0
14	0.0014	0.0002182	0.0018938	8.28e-5	-11.0892019
16	0.00141	0.0002467	0.00184	8.98e-5	-13.6150235
18	0.001255	0.0001285	0.00184	7.92e-5	-13.6150235
20	0.001496	0.00021	0.0019703	9.62e-5	-7.49765258

Fig. 22. Plot between strains versus time for different vanes

(a)

(a)

(b)
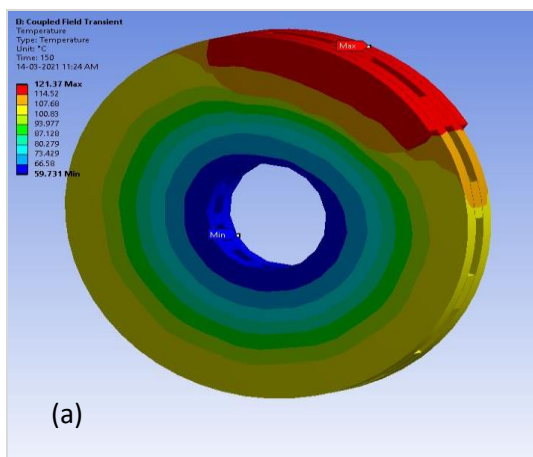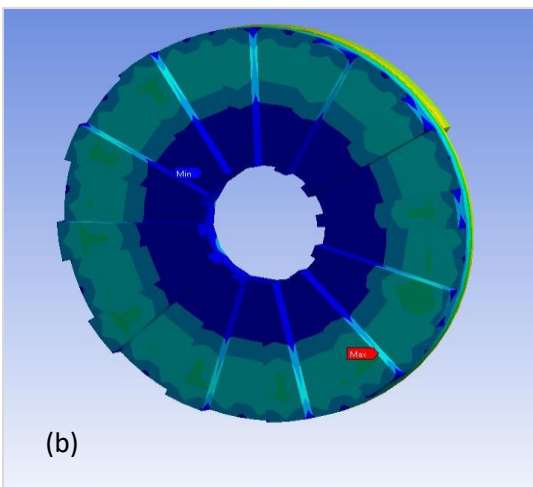
(b)

Fig. 23. Temperature distribution in disc brake with 12 vanes (a) 150th Sec (b)12th Sec
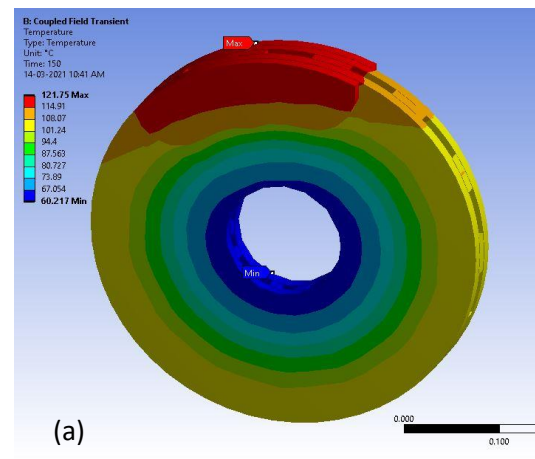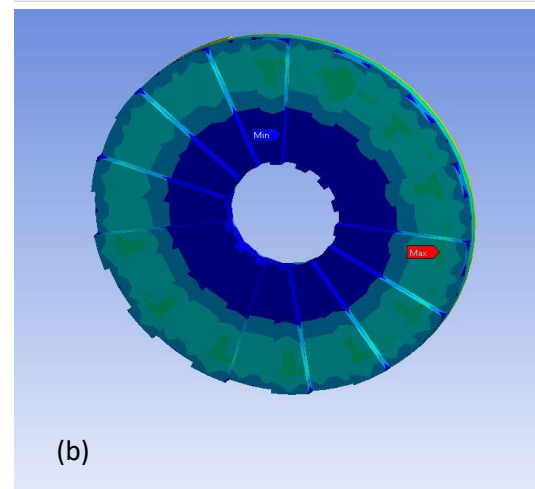
Fig. 24. Temperature distribution in disc brake with 14 vanes (a)150th Sec (b) 12th Sec

3.4.3. 16 Vanes

After a stimulation of 150 seconds in the disc with 16 vanes, it is seen in Figure 25 (a) that a maximum of 122.17 °C and a

minimum 60.714 °C occur at the point indicated in below image. During the whole stimulation, it is seen in Figure 25 (b) that a maximum 268.87 °C and a minimum of 25°C occur at 12th second.

3715

(a)

(b)

Fig. 25. Temperature distribution in disc brake with 16 vanes (a)150th Sec (b) 12th Sec
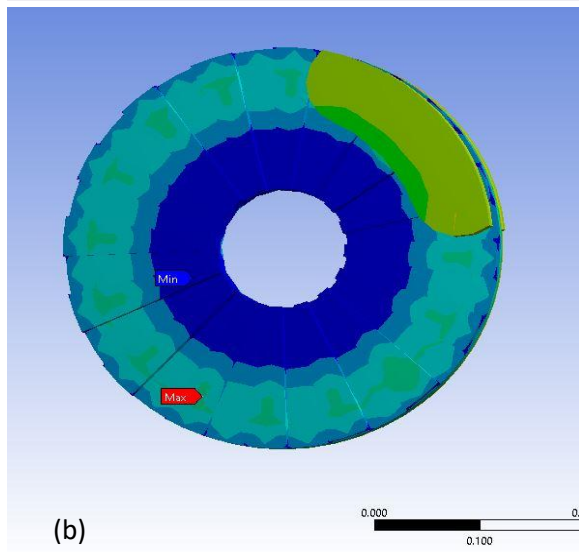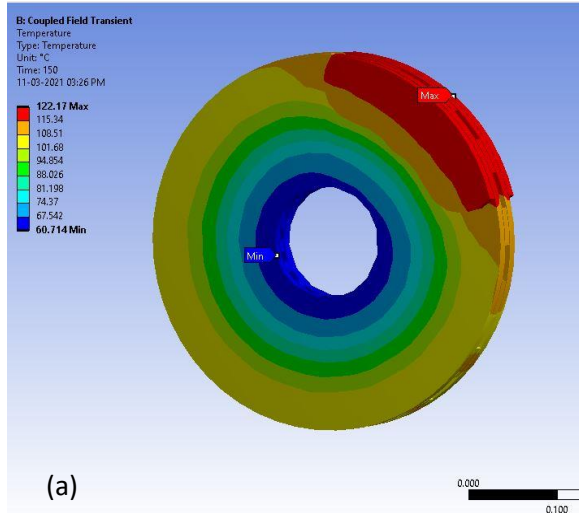

(a)

(b)

Fig. 26 Temperature distribution in disc brake with 18 vanes (a)150th Sec (b)15th Sec

3.4.4. 18 Vanes

After a stimulation of 150 seconds in the disc with 18 vanes, it is seen in Figure 26 (a) that a maximum of 126.88 °C and a minimum 61.059 °C occur at the point indicated in below image. During the whole stimulation, it is seen in Figure 26 (b) that a maximum 270.17 °C and a minimum of 25°C occur at 15th second.
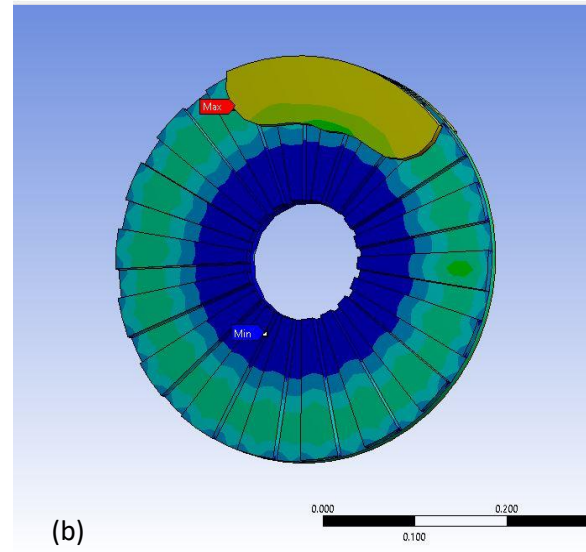
3.4.5. 20 Vanes

After a stimulation of 150 seconds in the disc with 20 vanes, it is seen in Figure 27 (a) that a maximum of 129.33 °C and a minimum 61.728 °C occur at the point indicated in below image. During the whole stimulation, it is seen in Figure 27 (b) that a maximum 272.83.17 °C and a minimum of 25°C occur at 13th second.
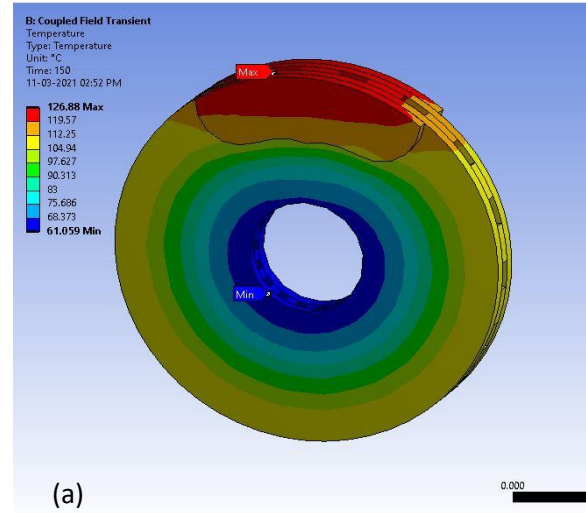
3.4.6. Comparisons

From the below graph (Figure 28), it can be seen that as the number of vanes increases from 12 vanes to 20 vanes, maximum temperature increases slightly.
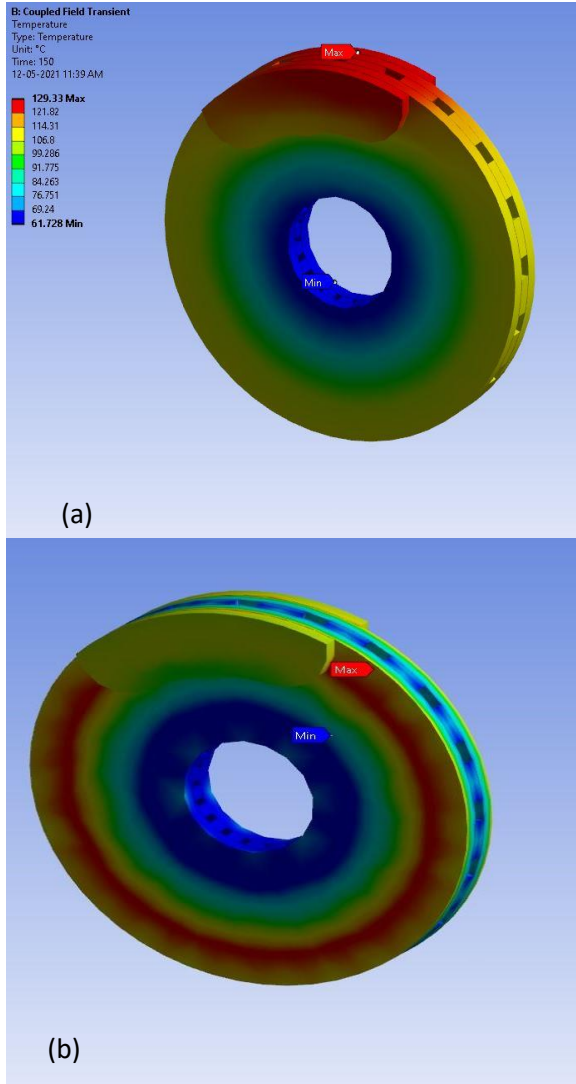
3716   Automotive Science and Engineering

(a)

(b)

Fig. 27. Temperature distribution in disc brake with 20 vanes (a)150th Sec (b)13th Sec

Table. 8. Comparison of temperatures of different vanes

No of Vanes	Temperature at 150 sec(°C)		Maximum Temperature (°C)	Minimum Temperature (°C)	% Change in Maximum Temperature (°C)
	Max	**Min**			
12	121.37	59.71	268.01	25	0
14	121.75	60.217	268.5	25	0.182828999
16	122.17	60.714	268.87	25	0.320883549
18	126.88	61.059	270.17	25	0.805940077
20	129.33	61.728	272.83	25	1.798440357

It is found that maximum temperature occurs in disc with 18 vanes. As the number of vanes increases, there is slight increase in the maximum temperature rise during the whole stimulation. From Table 8, it is clear that disc rotor with 20 vanes has highest maximum temperature rise among all 5 designs and has 1.79% more than maximum temperature rise of disc rotor with 12 vanes.

4. Conclusions

In this study, both thermal and mechanical loads are applied simultaneously in transient conditions. Five models of ventilated disc brake with 12,14,16,18 and 20 vanes are stimulated for 150 seconds in each case. From this study, it is observed that as the number of vanes increases from 12 to 18, there is minor reduction in the maximum deformation and a significance reduction in maximum stress and maximum strain is observed. An increase in maximum deformation, maximum stress and maximum strain is noticed when number of vanes increase from 18 to 20. In temperature distribution a slight increase in the maximum temperature is seen as the number of vanes increase from 12 to 20. A decrease of 3.87% in maximum deformation, 15.49% in maximum stress and 13.61% in maximum strain is noted in disc brake with 18 vanes as compared to disc brake with 12 vanes. It can be concluded from this study that disc brake with 18 vanes is best suitable design among all design tested. It is observed that increasing the number of vanes beyond 18 has an opposite effect on the performance of disc brake.
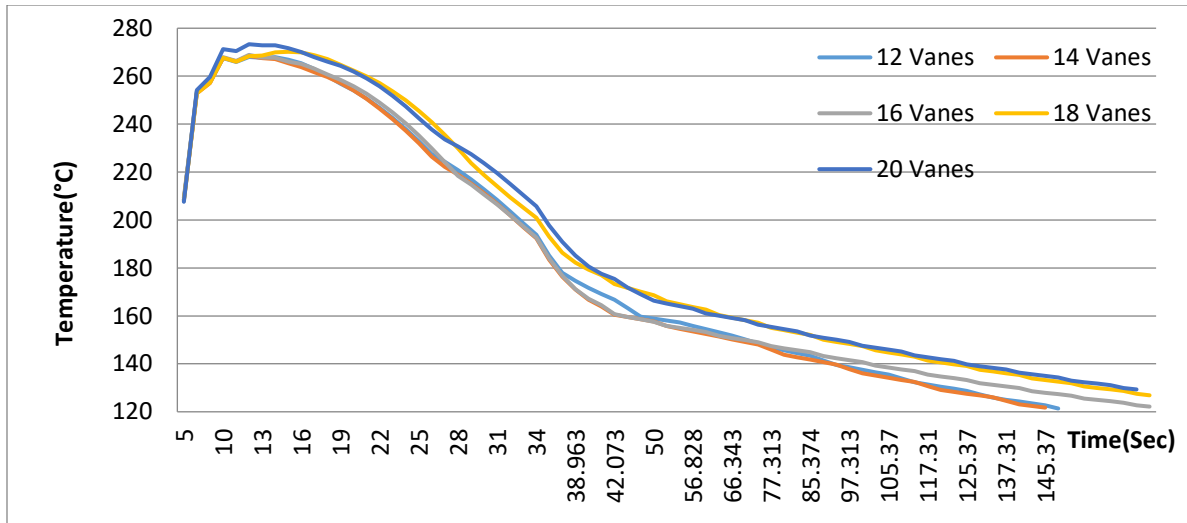
3717

Fig. 28. Plot of temperature distribution in disc brake with different vane

References

[1]   Yevtushenko, A. A., and P. Grzes. "3D FE model of frictional heating and wear with a mutual influence of the sliding velocity and temperature in a disc brake." *International Communications in Heat and Mass Transfer* 62 (2015): 37-44

[2]   Belhocine, A., and O.I. Abdullah. "Design and thermomechanical finite element analysis of frictional contact mechanism on automotive disc brake assembly." *Journal of Failure Analysis and Prevention* 20, no. 1 (2020): 270-301.

[3]   Pevec, M., I. Potrc, G. Bombek, and D. Vranesevic. "Prediction of the cooling factors of a vehicle brake disc and its influence on the results of a thermal numerical simulation." *International Journal of Automotive Technology* 13, no. 5 (2012): 725-733.

[4]   Jian, Q,, and Yan S. "Numerical and experimental analysis of transient temperature field of ventilated disc brake under the condition of hard braking." *International Journal of Thermal Sciences* 122 (2017): 115-123.

[5]   Guo, F., Y. Yan, Y. Hong, and Y. Li. "Multiscale modeling: Prediction for thermophysical properties of needled carbon/carbon composite and evaluation of brake disk system." *Materials Today Communications* 22 (2020): 100685.

[6]   Yan, H., W.-T. Wu, S. Feng, and G. Xie. "Role of vane configuration on the heat dissipation performance of ventilated brake discs." *Applied Thermal Engineering* 136 (2018): 118-130.

[7]   Yan, H. B., S. S. Feng, X. H. Yang, and T. J. Lu. "Role of cross-drilled holes in enhanced cooling of ventilated brake discs." *Applied Thermal Engineering* 91 (2015): 318-333.

[8]   Yevtushenko, A., M,Kuciej, E. Och, and O. Yevtushenko. "Frictional heating of the brake disc with essential nonlinearity thermal barrier coating." *International Communications in Heat and Mass Transfer* 95 (2018): 210-216.

[9]   Belhocine, A., and M. Bouchetara. "Investigation of temperature and thermal stress in ventilated disc brake based on 3D thermomechanical coupling model." *Ain Shams Engineering Journal* 4, no. 3 (2013): 475-483.

[10]   Chen, A., and F.Kienhöfer. "The failure prediction of a brake disc due to nonthermal or mechanical stresses." *Engineering Failure Analysis* (2021): 105319.

[11]   Kishore, V. S. N., and K. P. Vineesh. "Temperature evolution in disc brakes during braking of train using finite

element analysis." *Materials Today: Proceedings* 41 (2021): 1078-1081.

[12]   Jian, Q., L.Wang, and Y.Shui. "Thermal analysis of ventilated brake disc based on heat transfer enhancement of heat pipe." *International Journal of Thermal Sciences* 155 (2020): 106356.

[13]   Pevec, M., G. Oder, I. Potrč, and M. Šraml. "Elevated temperature low cycle fatigue of grey cast iron used for automotive brake discs." *Engineering Failure Analysis* 42 (2014): 221-230.

[14]   Gigan, G., V. Norman, J.Ahlström, and T.Vernersson. "Thermomechanical fatigue of grey cast iron brake discs for heavy vehicles." *Proceedings of the Institution of Mechanical Engineers, Part D: Journal of Automobile Engineering* 233, no. 2 (2019): 453-467.

[15]   Ripley, M. I., and O. Kirstein. "Residual stresses in a cast iron automotive brake disc rotor." *Physica B: Condensed Matter* 385 (2006): 604-606.

[16]   Maluf, O., M. Angeloni, M. T. Milan, D. Spinelli, W. Wladimir, and B.Filho. "Development of materials for automotive disc brakes." *Minerva* 4, no. 2 (2007): 149-158.

[17]   Manocha, L. M. "High performance carbon-carbon composites." *Sadhana* 28, no. 1 (2003): 349-358.

[18]   Kumar, P., and V. K. Srivastava. "A review on wear and friction performance of carbon–carbon composites at high temperature." *International Journal of Applied Ceramic Technology* 13, no. 4 (2016): 702-710.

[19]   P. Cook, "Conditions for string stability," *Systems & control letters,* vol. 54, pp. 991-998, 2005.

[20]   Yevtushenko, A., M.Kuciej, and P.Wasilewski. "Experimental study on the temperature evolution in the railway brake disc." *Theoretical and Applied Mechanics Letters* 9, no. 5 (2019): 308-311.

[21]   Chen, G. X., J. Z. Lv, Q. Zhu, Y. He, and X. B. Xiao. "Effect of the braking pressure variation on disc brake squeal of a railway vehicle: Test measurement

and finite element analysis." *Wear* 426 (2019): 1788-1796